ISTANBUL UNIVERSITY PRESS

RESEARCH ARTICLE

Eur J Biol 2022; 81(2): 240-250

Epibrassinolide Triggers Apoptotic Cell Death in SK-N-AS Neuroblastoma Cells by Targeting GSK3β in a ROS Generation-Dependent Way

Pinar Obakan Yerlikaya[1,2], Shafaq Naxmedova[3]

[1]Istanbul Medeniyet University, Faculty of Engineering and Natural Sciences, Department of Molecular Biology and Genetics, Uskudar-Istanbul, Turkiye
[2]Istanbul Medeniyet University, Science and Advanced Technology Research Center, Uskudar-Istanbul, Turkiye
[3]Istanbul University, Aziz Sancar Institute of Experimental Medicine, Department of Genetics, Istanbul, Turkiye

ORCID IDs of the authors: P.O.Y. 0000-0001-7058-955X; S.N. 0000-0002-2288-8296

Please cite this article as: Obakan Yerlikaya P, Naxmedova S. Epibrassinolide Triggers Apoptotic Cell Death in SK-N-AS Neuroblastoma Cells by Targeting GSK3β in a ROS Generation-Dependent Way. Eur J Biol 2022; 81(2): 240-250.
DOI: 10.26650/EurJBiol.2022.1191701

ABSTRACT

Objective: Epibrassinolide (EBR), a biologically active member of the brassinosteroids plant hormone family, has been recently indicated as an apoptotic inducer in various cancer cells without affecting non-tumor cell proliferation. Glycogen synthase kinase 3β (GSK3β) was the first identified molecule that acts as a critical mediator of glycogen metabolism and insulin signaling mechanism. GSK3β has been described as an essential factor for tumor progression by phosphorylating and inactivating the pro-apoptotic family member of the Bcl-2 family, Bax. It was recently shown to regulate cell division, differentiation, and adhesion.

Materials and Methods: To investigate the relative cell viability affected by EBR treatment and the preventive effect of N-acetyl cysteine (NAC) we performed MTT assay and FACS analysis, respectively. Colony formation and soft agar techniques were used to understand the inhibitory effect of EBR on colony formation and diameters. Annexin V-PI analysis by flow cytometry was performed for the measurement of the apoptotic cell percentages. Fluorescence microscopy was performed for the determination of mitochondria membrane potential following DiOC6 staining. The expression profiles of apoptotic proteins, as well as GSK3β and β-catenin were investigated by immunoblotting.

Results: Our results indicated that EBR induced mitochodria-mediated apoptosis by inducing ROS generation which can be prevented by NAC, a reactive oxgen species scavenger. EBR-induced apoptosis can influence the inhibitory phosphorylation of GSK3β by Ser9 and prevents the translocation of the down-stream target, β-catenin.

Conclusion: This study evaluated EBR as a potential apoptotic inducer in neuroblastoma cell line SK-N-AS and investigated the GSK3β involvement.

Keywords: Neuroblastoma, epibrassinolide, GSK3β, reactive oxygen species

INTRODUCTION

Neuroblastoma is a common extracranial solid tumor in childhood formed due to the neoplastic transformation of neural crest cells. Tumors are present in the tissues that form the sympathetic nervous system, mainly the adrenal gland (1). The cancer staging varies between the regressing tumors to highly metastatic and mortal ones due to poor prognosis and molecular signatures, including the *MYCN* gene, the most critical genetic marker of neuroblastoma aggressiveness (2). Treatment strategies mostly require chemotherapy, especially for the high-risk group, consisting of platinum derivatives, alkylating, and topoisomerase-inhibitor agents. In ad-

Corresponding Author: Pinar Obakan Yerlikaya E-mail: pinar.obakan@medeniyet.edu.tr
Submitted: 19.10.2022 • **Accepted:** 22.11.2022 • **Published Online:** 15.12.2022

Content of this journal is licensed under a Creative Commons Attribution-NonCommercial 4.0 International License.

dition, in the case of ALK tyrosine kinase mutation in existing tumors, ALK inhibitor crizotinib is usually preferred (3). In recent years, glycogen synthase kinase 3 (GSK3) inhibitors have been used to reduce neuroblastoma cell growth and markers (4). Even ALK and GSK3 kinase inhibitors showed promising results in inducing apoptosis in neuroblastoma cell lines and in vivo mice models (5). Besides its role in glycogen synthesis, GSK3 performs critical functions in various cellular processes, including apoptosis, cell growth, invasion, and metastasis. Therefore, aberrant GSK3 activity is associated with many diseases, such as cancer (6). Several GSK3 inhibitors have been developed and are being tested in clinical trials (7).

Brassinosteroids (BRs) were first obtained from plant pollen of the genus Brassica. The first identified member of BRs, brassinolide, was isolated from pollen in the form of crystals and was the first plant component in steroid structure (8). BRs are natural polyhydroxy steroids found in vertebrates and insects, similar to steroid hormones (9). Their roles, such as embryonic and post-embryonic development and maintaining the organism's homeostasis, have been identified in animals. In plants, BRs control many physiological events. It has been shown that BRs are essential in regulating many events in plant development, especially in seed germination, root and stem development, vascular differentiation and fertility, and salinity and metal stress management (10). Recent studies have shown that Epibrassinolide (EBR) has the potential to induce apoptotic cell death in cancer cells (11). Due to the structural similarity, the first studies focused on the nuclear hormone receptor (NHR) action during cancer cell apoptosis (12). However, our group has shown that EBR-induced apoptosis occurred in NHR-expressing and non-expressing cell lines (13,14).

In this study, we showed that EBR induced pGSK3β phosphorylation by Ser9 and inhibited the translocation of its downstream target β-catenin. EBR treatment triggered cell viability loss via mitochondria-mediated and caspase-dependent apoptosis in SK-N-AS cells. Moreover, we showed that EBR-induced apoptosis mainly occurs due to endoplasmic reticulum stress induction. Our recent findings also suggested that EBR is a candidate GSK3β inhibitor in a low concentration and induces apoptosis in SK-N-AS cells and GSK3β inhibition acting on the Ser9 phosphorylation domain may be important for this phenomenon.

MATERIALS AND METHODS

Drug and Antibodies

24-epibrassinolide was purchased from Apollo Scientific (Stockport, Cheshire, UK), dissolved in DMSO to make a 10 mM stock solution, and stored at -20˚C. Bax, Bcl-2, Puma, Bid, cleaved caspase 3, cleaved caspase 7, pro-caspase 9, cleaved poly (ADP-ribose) polymerase (PARP), GSK3β, phospho- GSK3β Ser9, and β-catenin Histone H3 rabbit primary antibodies (each diluted 1:1,000) were purchased from Cell Signaling Technology (CST, Danvers, MA, USA). Horseradish peroxidase (HRP)-conjugated secondary anti-rabbit antibodies (diluted 1:3,000) were from CST.

Cell Culture

SK-N-AS cell line was obtained from American Type Tissue Culture Collection and was grown in DMEM medium supplemented with 10% fetal bovine serum, 1% 10 U/ml penicillin/streptomycin, and 1% non-essential amino acids. Cells were kept in a 5% CO_2 incubator at 37 ºC (Heracell 150; Thermo Electron Corporation, Waltham, MA, USA).

MTT Assay

The effect of EBR on cell viability was determined by colorimetric 3-(4,5-dimethylthiazol-2-yl)-2,5-diphenyl-tetrazolium bromide (MTT; Roche, Indianapolis, IN, USA) assay. Cells were seeded at a density of $1x10^4$ cells/well in 96-well plates, allowed to attach overnight, and treated with the increasing concentrations of EBR (0-30 µM) for 24 h. After the treatment, 10 µl of MTT reagent (5 mg/ml) was added to the cell culture medium for 4 h. Following the removal of media, 200 µl DMSO was added to dissolve the formazan crystals. The absorbance of the suspensions was determined at 570 nm with a microplate reader (Bio-Rad, Hercules, CA, USA).

Trypan Blue Dye Exclusion Assay

Cells were seeded on 6-well plates ($5x10^4$ cells/well) and treated with increasing doses of EBR (0-10 µM) for 96 h. Every 24 h, the cells were trypsinized and stained with trypan blue. Data were plotted on a graph indicating the number of cells (y-axis) vs time (x-axis). Viable and dead cells were counted under light microscopy.

Colony Formation Assay

SK-N-AS cells were seeded at a density of $5x10^3$/well in a 6-well petri dish. Following overnight attachment, cells were treated with 1 and 10 µM EBR for 24 h. The drug-containing media were removed, and cells were allowed to form colonies in complete media for 10 days. The colonies were fixed with a solution of acetic acid and methanol (1:3) for 5 min. The supernatant was removed. Later, cells were stained with 0.5% crystal violet for 30 min at room temperature. Finally, the dye was washed away with distilled water, and the colonies were visualized under the light microscope.

Soft Agar Colony Formation Assay

5% agarose was first prepared and autoclaved. For the bottom agar, 500 µl of 5% agarose and 500 µl of DMEM medium containing 20% fetal bovine serum (FBS) were mixed and poured into a 6-well petri dish. The agar was kept in laminar flow until polymerization. 3% agarose was mixed with media containing 20% FBS and pipetted. The medium containing 10% FBS and 2500 cells were added to the mixture, pipetted, and poured into Petri dishes. For treated samples, a drug was added to this mixture. The petri dish was kept in a 5% CO_2 incubator at 37ºC for 10 days. After 10 days, colonies were examined under a light microscope.

Fluorescence Microscopy

Propidium Iodide Staining

$1x10^4$ cells were seeded in 6-well petri dishes and allowed to adhere overnight. 1 and 10 µM EBR was applied for 24 h. After the

incubation period, the medium was discarded, and the cells were incubated with a DMEM medium containing propidium iodide (P.I.) for 30 min. At the end of this period, the medium containing P.I. was discarded, and cells were washed with 1x PBS. After adding 500 µl of 1x PBS to each well, cells were examined under a fluorescent microscope (Excitation: 536 nm, Emission: 617 nm).

3,3'Dihexyloxacarbocyanine Iodide (DiOC6) Staining

SK-N-AS ($1x10^5$) cells were seeded into 12-well plates. Following exposure of cells to EBR (1 and 10 µM), they were washed once with 1X PBS and then stained with 4 nM 3,3'-dihexyloxacarbocyanine iodide (DiOC6) (40 nM stock concentration in DMSO; Calbiochem, La Jolla, CA, USA) fluorescent probe. The disruption of mitochondrial membrane potential (MMP) was visualized by fluorescence microscopy (excitation: 488 nm, emission: 525 nm).

4',6-diamidino-2-phenylindole (DAPI) Staining

The cells were seeded in 12-well plates at a density of $1x10^5$ cells/well and treated with increasing concentrations of EBR for 24 h. Cells were stained with 1 µl/ml DAPI (1 mg/ml stock concentration in 1X PBS) fluorescent probe and were incubated for 10 min in the dark. Nuclear DNA fragmentation was visualized using fluorescence microscopy (excitation: 350 nm emission: 470 nm).

2',7'-dichlorofluorescein-diacetate (DCFH-DA) Staining

DCFH-DA was used to monitor reactive oxygen species (ROS) production in EBR-treated cells. SK-N-AS cells were seeded at a density of $1x10^4$ cells/well in a 6-well petri dish. 1 and 10µM EBR were applied for 24 h. 1 µM DCFH-DA in fresh media were added to each well following the incubation period and washing step with 1x PBS. Cells were kept dark for 5'. After the washing step with 1x PBS, 500 µl of PBS was added to each well, and the oxidized form of DCFH-DA was examined under the fluorescence microscope at 480 nm excitation and 500 nm emission wavelengths.

Immunoblotting

SK-N-AS cells were treated with the appropriate concentrations of EBR in a time-dependent manner. First, all the samples were washed with ice-cold PBS and lysed on ice in a solution containing 20 mM Tris-HCl (pH 7.5), 150 mM NaCl, Nonidet P-40 0.5%, (v/v), 1 mM EDTA, 0.5 mM PMSF, 1 mM DTT, and protease inhibitor cocktail (Complete, Roche). After cell lysis, the cell debris was removed by centrifugation for 15 min at 13,200 rpm, and protein concentrations were determined by the Bradford protein assay (BioRad). ProteoJET protein isolation kit was used for cytoplasmic and nuclear protein isolation. Cells were seeded in 100 mm Petri dishes at a density of $3x10^6$ cells. Following EBR treatment for 24 h, cells were trypsinized and centrifuged at 600 g for 5 min. The nuclear and cytoplasmic protein isolation was performed according to the manufacturer's instructions. Samples were kept in the -80° freezer until use. Total, nuclear, and cytoplasmic protein lysates were separated on a 12% SDS-PAGE and transferred onto PVDF membranes (Roche). The membranes were then blocked with 5% milk blocking solution in Tris buffer saline-Tween 20 and incubated with appropriate primary and HRP-conjugated secondary antibodies (CST) in antibody buffer containing 5% (v/v) milk blocking solution. Following a gentle washing step with 1X TBS-Tween 20, the proteins were analyzed using an enhanced chemiluminescence detection system.

Flow Cytometry

Determination of Apoptotic Cell Death by Annexin V and Propidium Iodide Staining

Apoptotic cell death was detected following EBR treatment by annexin V-PI staining (B.D. Biosciences). The protocol was performed according to the manufacturer's instructions. Briefly, cells were mixed in 500 µl annexin V binding buffer, then incubated with 5 µl annexin V–FITC and 5 µl P.I. (50 µg/ml) for 10 minutes after centrifugation in the dark and at room temperature. $1x10^4$ cells per sample were analyzed by flow cytometry. Cells are presented as dots in a rectangular plot, with annexin V fluorescence in the x- and P.I. fluorescence on the y-axis. The numbers in each panel of the quadrant represent the % of the cell population as healthy (lower-left), early apoptotic (lower-right), late apoptotic (upper-right), and necrotic (upper-left) populations. The analysis of the obtained data was carried out using the BD Accuri C6 program.

Determination of the ROS Generation by DCFH-DA Staining

SK-N-AS cells were seeded in 6-well plates ($1x10^5$ cells/well). Cells were trypsinized, resuspended in 1X PBS, and stained with DCFH-DA (1 µM) (Molecular Probes, Inc., Eugene, OR, USA) for 15 min in a 5% CO_2 incubator. After the incubation period, DCFH-DA was added and flow cytometry analysis was performed (B.D. Biosciences, Accuri C6). Following exposure of cells to EBR for 24 h, media was carefully discarded.

Cell Cycle Analysis by PI Staining

Cells at a density of $2x10^5$ cells/well were seeded in 6-well plates and then treated with EBR. Both floating and adherent cells were collected and fixed with 70% ethanol. After incubation on ice for 30 min, the cells were diluted with 1X PBS. Samples were then centrifuged at 1,200 rpm for 5 min. Pellets were resuspended in 1X PBS, RNase (100 µg/ml), and PI solution (40 µg/ml). Samples were kept for 30 min at 37˚C in the dark. Cell cycle distribution was analyzed by Accuri C6 (B.D. Biosciences, Oxford, U.K.). 10,000 events/samples were acquired and evaluated using BD Accuri C6 software (B.D. Biosciences).

Statistical Analysis

All the experiments were statistically analyzed by two-way ANOVA using GraphPad Prism 9 (GraphPad Software, La Jolla, CA, USA). Error bars in the graphs were generated using ± standard deviation (S.D.) values. Statistically significant results by ANOVA were further analyzed by Bonferroni posthoc analysis. A $p<0.05$ was considered to indicate a statistically significant result.

RESULTS

EBR Treatment Diminished the SK-N-AS Cell Viability

The MTT test determined the effect of EBR on SK-N-AS cell viability. As seen in Figure 1A, the relative viability percentages of EBR-treated cells decreased dose-dependent. The percentage of relative viability after 24 h of 1µM EBR treatment was 67.7%.

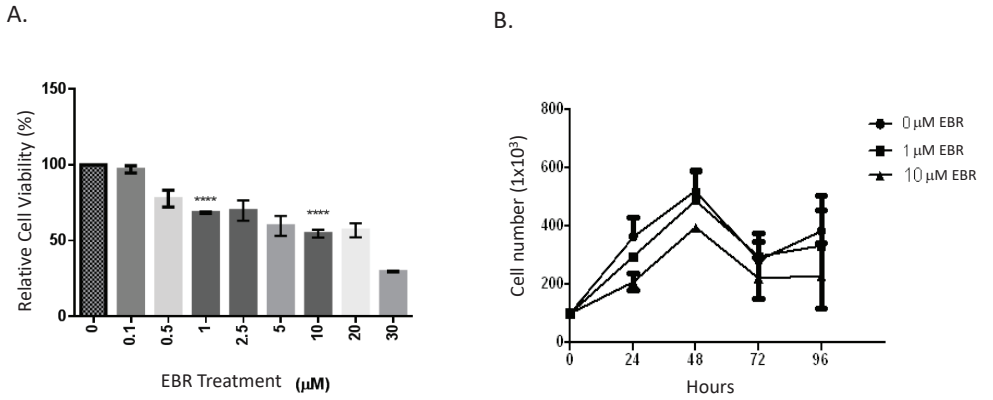

Figure 1. **A.** Investigation of dose-dependent cell viability of EBR in SK-N-AS cells by MTT method. ****p<0.00001. **B.** Determination of the effect of EBR on cell survival in SK-N-AS cells. Cells were treated with 1 and 10μM EBR for 24-96 h, and after staining with trypan blue, the cells were counted under a light microscope with the help of a Neubauer hemocytometer.

After 10 μM EBR treatment, the viability percentage dropped to 50.3%. (****p<0.00001). In addition, the effect of EBR on the SK-N-AS cell survival was also examined by trypan blue dye exclusion assay. Figure 1B indicates that EBR exerted a cytostatic effect rather than a cytotoxic one in concentrations 1 and 10 μM, time-dependently. 48 h EBR treatment dramatically prevented the survival of SK-N-AS cells.

EBR Inhibited the Clonogenic Potential of SK-N-AS Cells

A clonogenic assay was performed to determine the effect of EBR on colony formation in SK-N-AS cells. The colony formation potential of SK-N-AS cells was prevented in EBR-treated cells in a dose-dependent manner compared to control samples (Figure 2A). In addition, a soft agar colony formation test was also performed. As shown in Figures 3 and 4, the diameter of the col-

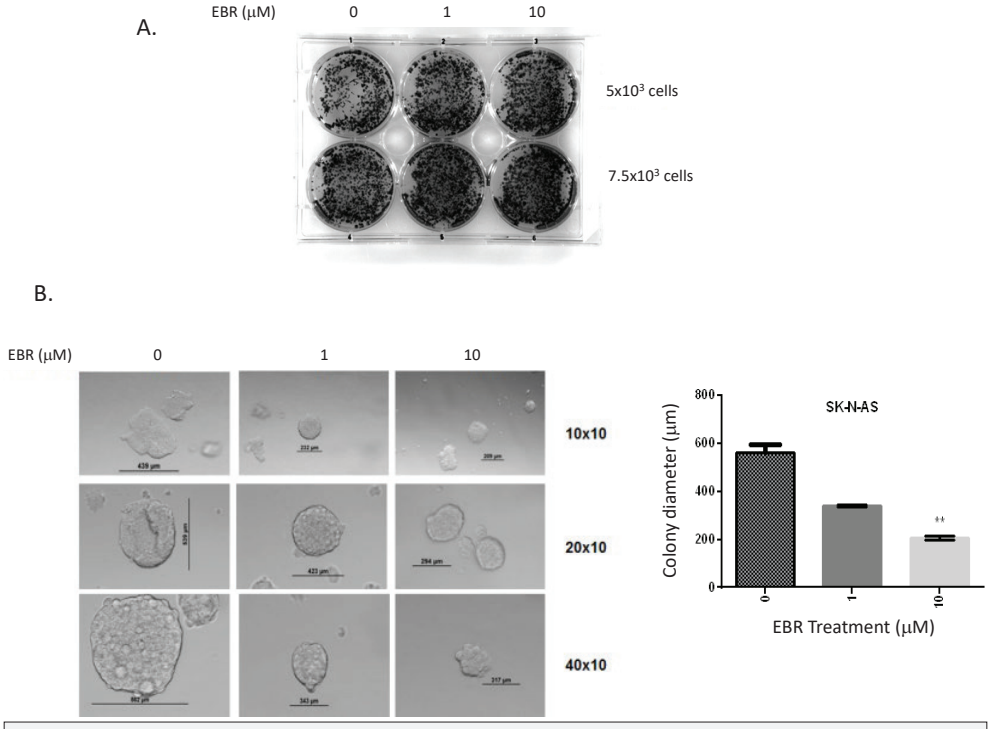

Figure 2. Investigation of the effect of EBR on colony formation in SK-N-AS cells. **A.** SK-N-AS cells were seeded in Petri dishes at 5x10³ and 7.5x10³ cells/well, 1 and 10μl of EBR were applied for 24 h, and the cells were incubated for 14 days. After 14 days, it was fixed and stained with crystal violet and images were taken under a light microscope**. B.** Investigation of colony formation on soft agar in SK-N-AS cells to which EBR had been applied. Cells incubated on soft agar for 10 days were examined under a light microscope at the end of 10 days, and colony diameters were measured. **p<0.01

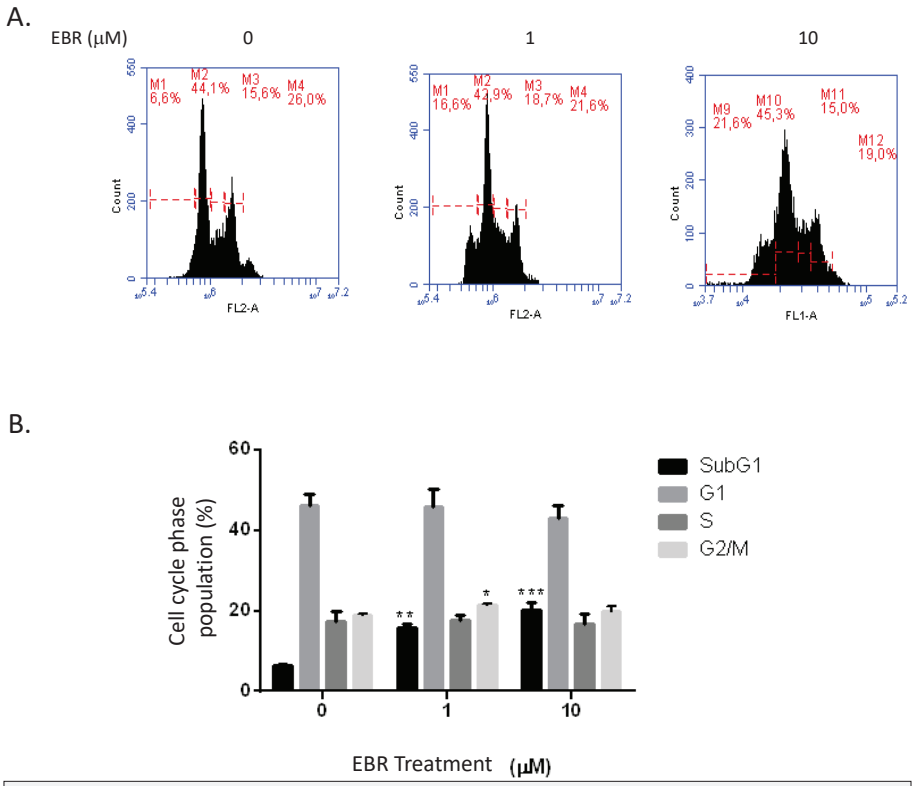

Figure 3. Flow cytometry analysis of cell cycle phases following exposure of SK-N-AS cells to EBR. **A.** Cells were incubated with EBR for 24 h, fixed with ethanol, and stained with PI. Flow cytometry was used for cell cycle analysis (Ex: 535 nm and Em: 617 nm). **B.** The number of cells in different cell cycle phases was determined after at least 3 repetitions of the experiment. Cell cycle distribution was analyzed by two-way ANOVA and Tukey's multiple comparisons test. *p <0.05, **p <0.01 and ***p <0.001

onies formed by the EBR-treated cells decreased depending on the dose. As seen in Figure 2B, a significant reduction in colony diameter was observed after 10 μM EBR treatment.

EBR Triggers Cell Cycle Arrest and Induced Apoptosis in SK-N-AS Cell Line

As seen in Figure 3A, an approximately 3-fold increase in the SubG1 population as a result of 24 h 1 μM EBR treatment was obtained in SK-N-AS cells, and an approximately 4-fold increase, as a result of 10μM EBR application. This result shows that EBR activates the apoptotic mechanism in SK-N-AS cells. In addition, the percentage of G2/M phase cells decreased by 25% with exposure of cells to 10 μM EBR (Figure 3B). Annexin V and PI staining were performed to determine whether apoptotic cell death was triggered in EBR-treated SK-N-AS cells. As seen in Figure 4, an approximately 15 fold higher total early and late apoptotic cell population was observed in cells treated with 1 μM EBR for 24 h, compared to the untreated control group. Cells treated with 10 μM EBR also exhibited an increased apoptotic population percentage, approximately 25 fold compared to the untreated samples. No significant change was found in the necrotic population. This result shows that EBR activates the apoptotic mechanism in SK-N-AS cells. Later, DiOC6 staining was performed to show mitochondria-mediated apoptotic cell death in the cell. Mitochondrial membrane potential is impaired in apoptotic cell death. For this reason, the dye cannot be retained in cells with the induction of apoptotic cell death. We found that both concentrations cause a decrease in the DiOC6 stained cell population, however, 10 μM EBR application was more effective to decrease DiOC6 staining compared to the 1 μM dose (Figure 5A). DAPI is a nucleic acid dye, which marks DNA fragmentation. Figure 5A clearly demonstrated the increase in DAPI staining inside the nucleus more specifically after 10 μM EBR treatment. We next checked the expression profiles of caspase and Bcl-2 family proteins playing a role in apoptosis induction using the immunoblotting technique. The changes in pro-and anti-apoptotic Bcl-2 family members, which have an essential role in mitochondria-mediated apoptotic cell death pathway, were investigated following EBR application. As seen in Figure 5B, Bid expression increased after 10 μM EBR treatment in SK-N-AS cells. Caspase-8 causes the proteolytic cleavage of Bid and causes Bid to migrate to mitochondria. Bid can bind to both Bax and Bcl-2, and it was observed that Bax expression increased as a result of 10 μM EBR application (Figure 5B). Bax resides in the cytosol and, upon apoptotic stimulation, binds to the mitochondrial membrane and induces pore formation. In addition, it was determined that the expression of PUMA protein increased

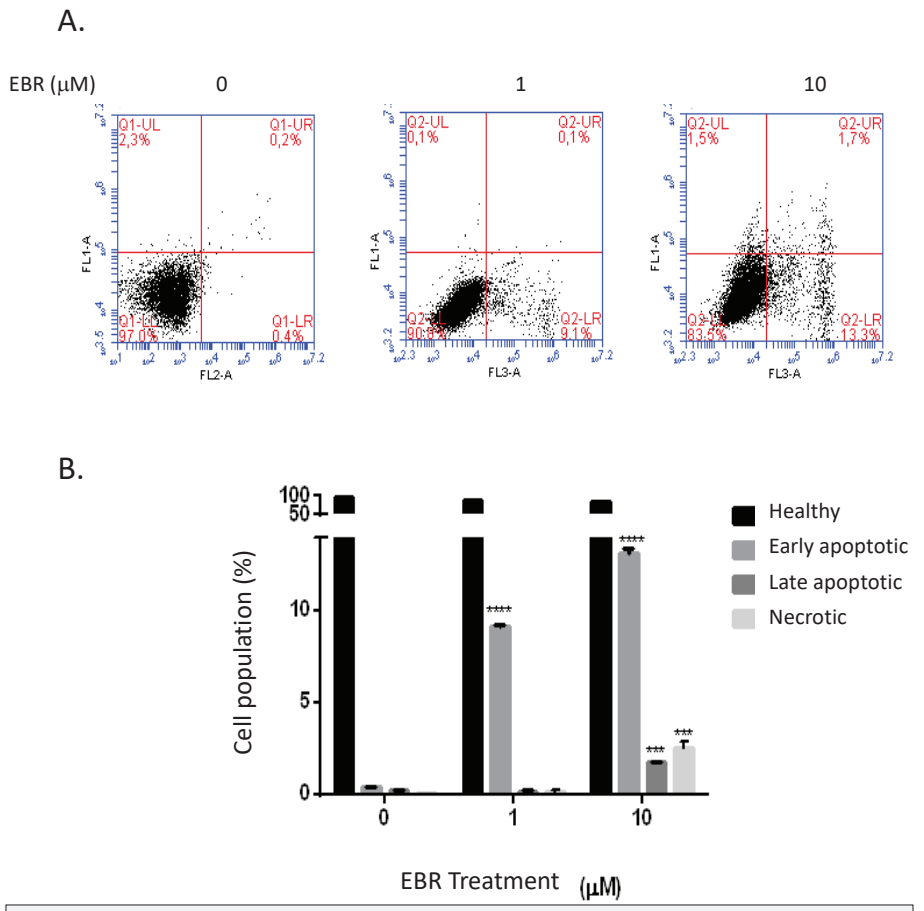

Figure 4. EBR induced apoptosis in SK-N-AS cells. **A.** After incubation with increasing concentrations of EBR for 24 h, cells were stained with Annexin V and PI and analyzed with FACS flow using the BD Bioscience Accuri C6 program. **B.** Percentages of early apoptotic, late apoptotic, and necrotic populations were determined after at least three independent experiments. ***p <0.001 and ****p <0.0001.

in SK-N-AS cells treated with 1 and 10 μM EBR for 24 h (Figure 5B). Puma stimulates apoptosis by binding to Bcl-2, promoting migration to mitochondria and releasing cytochrome c. It is seen in the data that the expression of the anti-apoptotic protein Bcl-2 protein is increased. As a result of 1 and 10 μM EBR application, no significant change was detected in the expression of Bcl-2 (Figure 5B). β-actin was used as a loading control.

Effective caspases cleave PARP, which is involved in DNA repair, causing apoptotic cell death. In addition to the Bcl-2 protein family, caspase family expressions in the apoptotic pathway were also investigated following EBR treatment in SK-N-AS neuroblastoma cells. The initiator caspase, procaspase-9, and the effective caspase-3 and caspase-7 expressions were determined. We found that the expression of the cleaved active form of PARP increased significantly in SK-N-AS cells after 1 and 10 μM EBR for 24 h (Figure 5B). Dose-dependent EBR treatment decreased procaspase-9 expression in the SK-N-AS cell line at 24 h. As a result of 1 and 10 μM EBR application, it was observed that the expression of cleaved caspase-3 and cleaved caspase-7 increased in SK-N-AS cells, confirming the apoptosis cell death (Figure 5B).

EBR Triggered ROS Generation Related to the Apoptotic Process in SK-N-AS Cells

To determine whether EBR affected ROS generation during the apoptotic induction in the SK-N-AS cell line, cells were treated with 1 and 10 μM EBR for 24 h and examined in flow cytometry following DCFH-DA staining. After diffusion into the cell, DCFH-DA is deacetylated by cellular esterases and then oxidized by ROS. As seen in Figure 5C, there was a significant increase in ROS in SK-N-AS cells treated with 1 and 10 μM EBR compared to control cells. N-acetyl cysteine (NAC), an agent that prevents the destructive effect of toxic agents in the apoptotic process triggered by EBR, was applied to SK-N-AS cells simultaneously with 10 μM EBR for 24 h, and changes in cell viability were observed. As seen in Figure 5D, NAC prevents the negative effect of EBR on cell viability in the SK-N-AS cell line and reverses the toxic effect of EBR (Figure 5D). In addition, NAC co-treatment also prevents EBR-induced ROS generation detected with DCFH-DA staining (Figure 5E).

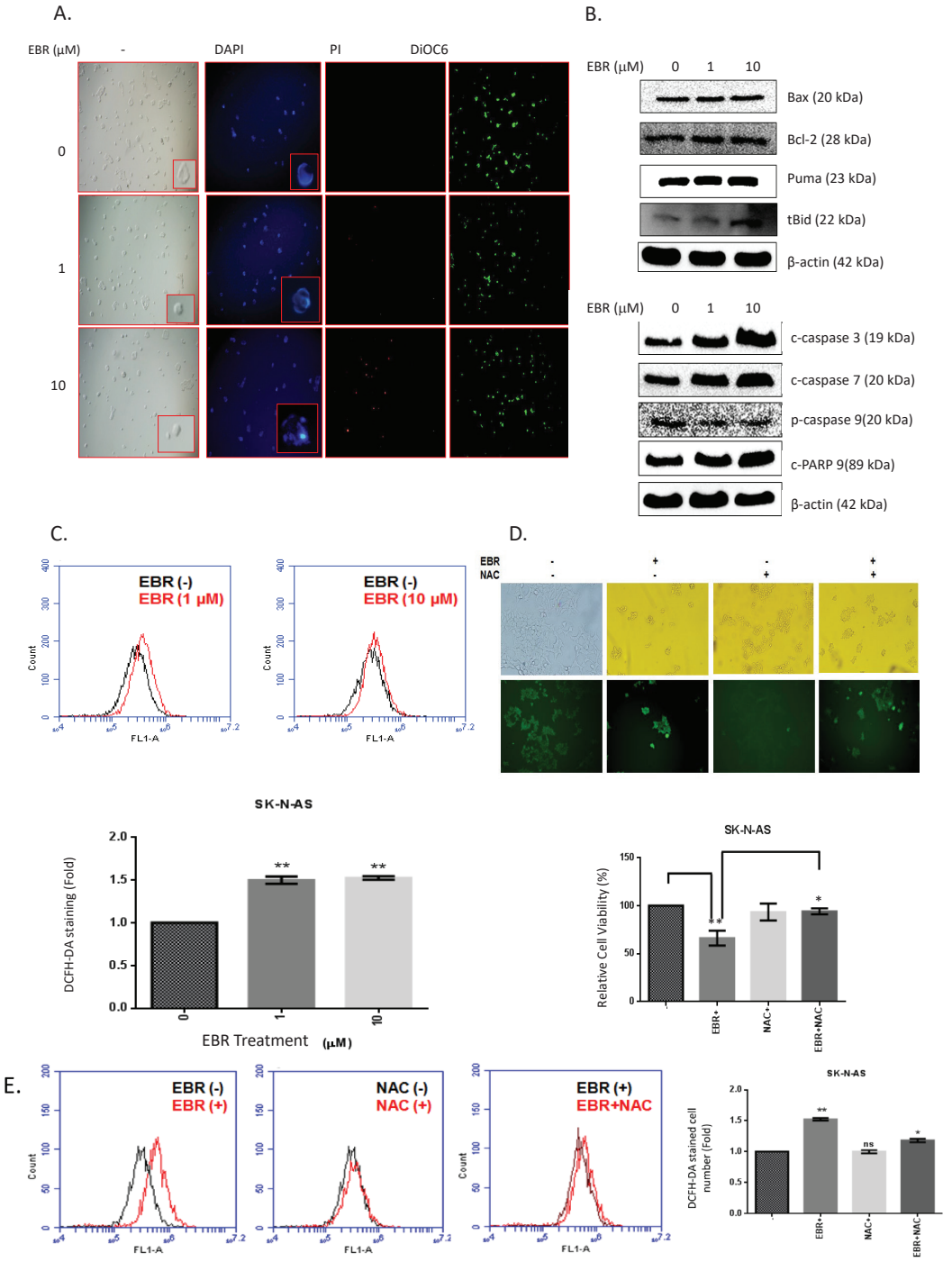

Figure 5. EBR-induced cell death was determined in SKNAS cells by fluorescent dyes. **A.** Cells treated with EBR for 24 h were later stained with DAPI, PI, and DiOC6, and examined under fluorescence microscopy (400x). **B.** 1 and 10 μM EBR was applied to SK-N-AS cells for 24 h. The immunoblotting method was used to determine the effects of EBR application on the pro-and anti-apoptotic Bcl-2 family, caspases, and PARP cleavage. After total protein isolation, 30 μg of protein was separated by 12% SDS-PAGE for each sample. The bands of the relevant proteins were determined based on the chemiluminescent feature. Beta-actin was used as the loading control. **C.** The effect of EBR treatment on ROS generation was determined after DCFH-DA staining. Cells were treated with 1 and 10 μM EBR for 24 h and then were stained with DCFH-DA. After 15 min of incubation, cells were analyzed by flow cytometry. **D.** The effect of NAC co-treatment with EBR on ROS generation was determined under fluorescence microscopy and by examining the cell viability loss with MTT assay. **E.** Co-treatment of NAC with EBR prevented ROS generation measured following FACS flow analysis. *p<0.05 and **p<0.01

Epibrassinolide Altered Wnt Signaling in SK-N-AS Cell Line

Wnt pathway proteins were examined in the SK-N-AS cell line. As seen in Figure 6A, a decrease was observed in the expression of GSK3β protein in SK-N-AS cells after 1 μM EBR for 24 h, in contrast, increased protein expression was observed following exposure of 10 μM EBR to the cell line (Figure 6A). We also detected the increased expression profile of the phosphorylated form of GSK3β by Ser9 residue, which indicates its inhibition after both 1 and 10 μM EBR treatments. The downstream target of GSK3β is β-catenin, an important transcription factor regulating various cellular processes including cell proliferation and cell cycle. As seen in Figure 6A, a decrease in the expression of the β-catenin protein was determined in SK-N-AS cells treated with 1 and 10 μM EBR for 24 h. In addition, the nuclear localization of β-catenin was also prevented more specifically following the exposure of cells to 10 μM EBR (Figure 6B).

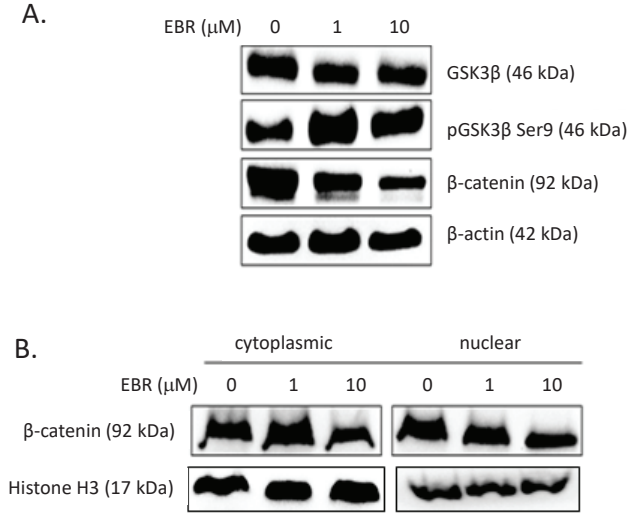

Figure 6. The effects of EBR were determined on GSK3/ β-catenin pathway. After **A.** total and **B.** nuclear-cytoplasmic protein isolation, 30 μg of protein was separated by 12% SDS-PAGE for each sample. After the immunoblotting procedures, the bands of the relevant proteins were determined based on the chemiluminescent feature. Beta-actin was used as the loading control.

DISCUSSION

Neuroblastoma, one of the deadliest tumors of infancy, is the malignancy of neural crest cells. The heterogeneity of the tumor-forming cells causes resistance to treatment, leading to metastatic spread and poor survival (15). Despite new interventions in therapeutic approaches, the current therapies are not effective and new treatment options are urgently needed since the overall survival rate is less than 10%. Previous studies have shown that GSK3β inhibition has been shown to reduce proliferation and increase apoptosis in neuroblastoma cells (4,5). The cell cycle arrest induced by lithium treatment has been shown to reduce cell proliferation in vitro in the B65 neuroblastoma cell line (4). Most importantly, similar effects were also observed in in vivo experimental set-ups, delayed tumor growth, and cell cycle arrest (16).

A potential GSK3 inhibitor EBR, similar to mammalian steroid hormones, belongs to the plant BR family, which has a vital role in plant growth and development. The cytotoxic effect of EBR was first identified in mammalian cancer cells. Later, the effect of EBR on nuclear hormone receptor (NHR) expressing cell lines was investigated, and it was concluded that EBR is a candidate for NHR expressing cells (12, 17). In this study, it was shown that EBR inhibited the cell cycle in the G1 phase in the estrogen-dependent MCF-7 breast cancer cell line, affecting the expression of CDKs (p21, p27, p53) and cyclins, which regulate the cycle and induced apoptosis (17). In 2014, our group demonstrated that EBR induced apoptosis in a p53-independent and caspase-dependent manner in both NHR expressing and non-expressing cancer cell lines, which pointed out another shared target between these cells (14). Intracellular proteomic changes were determined for this purpose by our group using the SILAC (stable isotope-labeled amino acid in cell culture) method (18). As a result of the study, our laboratory showed that many proteins related to cell survival, apoptosis, endoplasmic reticulum (ER) stress, and ubiquitination in cells exposed to EBR application were significantly altered compared to untreated control cells. Among these proteins, the most significant change was observed for calreticulin, which is a chaperone having a role in protein folding in the ER lumen and Ca^{2+} ion buffering (18). ER stress is defined as the accumulation of un/misfolded proteins in the ER lumen and the stress is often transmitted to the nucleus to start the cellular adaptation processes, including the induction of the transcription of chaperone proteins, or autophagy to eliminate misfolded proteins (19,20). However, ER stress can also initiate apoptosis if the recovery of cells in terms of protein folding is not achieved. The regulation of ER stress-induced apoptosis has been shown to involve GSK3 (21). GSK3 has two Ser/Thr kinase isoforms (GSK3α and GSK3β) with distinct roles and they are controlled by the inhibitory phosphorylations through Ser21 and Ser9, respectively (22). Following the activation of the Wnt signaling pathway, GSK3 associates with Axin to phosphorylate β-catenin and prepare it for proteasomal degradation (23). On the other hand, PI3K/Akt pathway activation can also lead to the inhibition of GSK3β, which in turn can influence the downstream target's (β-catenin) translocation to the nucleus (24). β-catenin was the first identified molecule having a role in cell-cell adhesion, in collaboration with E-cadherin (25). A significant relationship was shown between β-catenin activity and apoptosis (26). According to previous studies, caspases target β-catenin during apoptotic events and cause the dismantling of the cell adhesion. On the other hand, the decrease of β-catenin nuclear translocation following inhibited Wnt signaling has been suggested as a marker of cell survival loss for several cells, including cancer and neuronal cells (27,28). Several studies suggested that GSK3 has an obligatory role in CHOP activation leading to ER stress-induced apoptosis by activating caspases (29). According to our previous results, EBR can act as a GSK3β inhibitor in low concentrations (30). Therefore, we investigated the possible outcomes of GSK3β inhibition in neuroblastoma cells in this study. We found that EBR treatment caused cell viability

loss and survival in SK-N-AS cells. The colony-forming potential of the cell was also prevented by EBR treatment at low concentrations of 1 and 10 mM. Like our previous findings, the apoptotic potential of EBR was also visualized in the neuroblastoma cell line. The cytostatic effect of EBR has been demonstrated in prostate and colon cancer cells at 10 and 20 μM doses. A dose of 30 μM EBR produced a cytotoxic effect in these cells. The effect on the clonogenic potential of SK-N-AS cells was not observed, although steroid-derived drugs, including bicalutamide, have been shown to inhibit colony formation in various cancer cell lines (31, 32). A significant increase in the early and late apoptotic population percentage was observed, confirming our recent results indicating EBR is an apoptotic inducer in different cancer cell lines. Apoptotic markers were investigated to understand whether the loss of cell viability induced by EBR is due to apoptotic cell death. Several studies also indicate that steroid-derived chemotherapeutics could cause DNA damage or DNA fragmentation (33). Similar to our previous results, in which EBR caused DNA fragmentation in prostate and colon cancer cells, EBR was also able to induce DNA fragmentation in SK-N-AS cells (13,14). EBR treatment also induced mitochondrial membrane potential loss and cell death. These results indicated the anti-cancer properties of EBR in neuroblastoma cells.

In the next stage of our study, SK-N-AS cells were examined in flow cytometry to determine whether EBR affects the formation of ROS in the apoptotic process. According to our results, ROS generation was significantly increased following each concentration of EBR treatment compared to control samples. These results suggest that cell death in EBR-treated SK-N-AS cells occurs by mitochondrial pathway-mediated apoptosis. When EBR was combined with N-acetyl cysteine (NAC) in SK-N-AS cells, its effect on ROS generation and cell viability was determined. Compared to EBR alone, the combination of EBR and NAC inhibited ROS generation and loss of cell viability in SK-N-AS cells. Based on this, it was concluded that EBR is an agent that causes the formation of ROS. NAC is an agent that plays a vital role in detoxifying glutathione and xenobiotics. It can detoxify free radicals and reactive electrophiles. In the study by Olivieri et al., it was stated that NAC protects cells from oxidative stress and cytotoxic-stimulating compounds in the SH-SY-5Y neuroblastoma cell line (34). In our study, although no cytotoxic effect of NAC on SK-N-AS cells was observed, it was observed that NAC reversed the cytotoxic effect of EBR when applied together with the drug. The EBR-induced cell death mechanism was identified as mitochondria-mediated apoptosis since we observed significant expression changes in pro- and anti-apoptotic protein levels. It was observed that the expression levels of Bax, truncated Bid, and Puma were increased in SK-N-AS cells compared to control cells following EBR treatment. Deprivation of pro-apoptotic proteins is one of the causes of drug insensitivity. Bax and Puma are pro-apoptotic proteins located in the cytosol that translocate to mitochondria with the induction of apoptosis. Bax and Puma are under the direct transcriptional control of p53 through their respective binding sites. They have been shown to increase cytochrome c release and caspase cleavage in vitro and in vivo. In this respect, the increase in the expression of both pro-apoptotic proteins was necessary for the apoptotic effect of EBR in SK-N-AS cells. Studies have also shown the effect of EBR on Bax and Puma in colon, prostate, and breast cancer cells (35). In addition, Bid protein is another pro-apoptotic protein that is induced by caspase 8 activation via the external apoptotic pathway and effective on the mitochondrial pathway. Studies in the literature have not shown any effect of EBR on the extrinsic apoptotic pathway. This effect is specific to SK-N-AS cells, and the activation of this pathway needs to be clarified in the future. This study also examined Bcl-2 expression as an anti-apoptotic Bcl-2 family member. No significant changes in Bcl-2 protein expression were found in SK-N-AS cells. In the study by Obakan et al., it was shown that the expression of pro-apoptotic proteins Bax, Puma, Bak, and Bim in the PC3 prostate cancer cell line increased with EBR treatment, while the expression of anti-apoptotic proteins Mcl-1 and Bcl-2 decreased (14). In the study by Steigerova et al., it was shown that the expression of anti-apoptotic proteins Bcl-X_L and Bcl-2 decreased, and the expression of Bax and Bid pro-apoptotic protein decreased with time-dependent EBR treatment in MCF-7 breast cancer cell line (17). It has been shown that the expression of the anti-apoptotic proteins Bcl-2 and Mcl-1 did not change in the MDA-MB-438 breast cancer cell line, the Bid pro-apoptotic protein was cleaved, and the expression of Bax pro-apoptotic protein decreased. We also evaluated the effect of EBR on caspase cleavage in the SK-N-AS cell line. The cleaved and active forms of caspase-3, caspase-7, and PARP in the SK-N-AS cell line were found upregulated, and decreasing pro-caspase-9 expression was observed. Although the effect of EBR on neuroblastoma cells is not known in the literature, caspase-3, -7, -9 and PARP cleavage was observed in DU145 prostate and MDA-MB-231 breast cancer cells in other studies conducted with cancer cells that do not express functional steroid hormone receptors (14,17).

It is well known that GSK3β can have a tumor-promoting or a tumor-inhibiting role, depending on the cancer cell type. The previous study by Dickey A. et al. showed that the inhibition of GSK3β can increase apoptosis by decreasing the expression of the anti-apoptotic proteins XIAP and Bcl-2 (5). The same study also suggested that a decrease in cell viability was determined by inhibiting GSK3β in Neuro-2A neuroblastoma cells, with the induction of apoptosis and cell cycle arrest. The conflicting effects of GSK3β on apoptosis are known; it inhibits extrinsic death receptor-mediated apoptosis while promoting the mitochondrial intrinsic apoptotic pathway. In a study by Petit-Paitel et al. in 2009, it was shown that inhibition of GSK3β activity in mouse TSM1 neuron cells prevents cell death by inhibiting mitochondrial membrane potential changes and subsequent caspase-9 and caspase-3 activation (36). In another study it was stated that overexpression of GSK3β induced a caspase-dependent apoptosis in neuronal cells via Nuclear Factor κB (NFκB) Signaling inhibition. Kotliarova et al. also determined that the inhibition of GSK3β causes the activation of oncogenic transcription factor c-myc, thus apoptosis and ultimately cytotoxicity, by stimulating pro-apoptotic factors such as Bax, Bim, and

tumor-necrosis-factor-associated apoptosis-stimulating ligand (TRAIL) (37). In our study, when cells are exposed to EBR, a decrease in the expression of GSK3β and subsequent increase in the phosphorylated form of GSK3β by Ser9 were observed, suggesting that EBR could inhibit GSK3β activity. Despite the inhibition of GSK3β, we found that β-catenin levels are downregulated in SK-N-AS cells after EBR treatment, especially with 10 mM EBR. Similarly, a decrease in expression of both cytoplasmic and nuclear β-catenin was observed in 10 μM EBR treated cells. Studies showed that inhibition of GSK3β leads to transcriptional activation of different target genes via β-catenin activation. For example, the activity of β-catenin has been shown related to increasing the number of neurons differentiating from neurospheres (38). The aberrant accumulation of β-catenin in tumors is considered associated with p53 inactivation, an important tumor suppressor. Sadot et al have shown that the overexpression of wild-type p53 down-regulated β-catenin in cancer cells is accompanied by the inhibition of its transactivation potential (39). They suggested that the link between p53 and β-catenin requires an active GSK3β and the down-regulation of β-catenin is mediated by the ubiquitin-proteasome system. In addition, various recent studies also indicated that the down-regulation of β-catenin is an important phenomenon to decrease tumorigenicity, however, it can promote epithelial-mesenchymal transition, which occurs during metastasis (40,41). Therefore, the possible effects of EBR on epithelial-mesenchymal transition and metastasis could be examined in future experiments.

CONCLUSION

The data obtained from this study clearly showed for the first time that EBR can act on GSK3b signaling and downstream targets, including β-catenin, and promote apoptosis in SK-N-AS neuroblastoma cells. The epithelial-mesenchymal transition and metastasis processes activated in response to EBR related to Wnt and β-catenin signaling are worth clarifying in the future. The obtained data also provides a basis for future studies regarding the therapeutic efficacy of EBR and its use in *in vivo* trials related to Wnt signaling.

Acknowledgements: We are thankful to Berkay Gurkan for technical assistance.

Ethics Approval Statement: All the experiments were performed using a commercially available cell line from ATCC. Neither human nor animal samples were used in this research.

Peer Review: Externally peer-reviewed.

Author Contributions: Conception/Design of Study- P.O.Y.; Data Acquisition- P.O.Y., S.N.; Data Analysis/Interpretation- P.O.Y., S.N.; Drafting Manuscript- P.O.Y., S.N.; Critical Revision of Manuscript- P.O.Y., S.N.; Final Approval and Accountability- P.O.Y., S.N.

Conflict of Interest: Authors declared no conflict of interest.

Financial Disclosure: We are thankful to Istanbul Kultur University Scientific Projects Support Center for supporting this study.

REFERENCES

1. Qiu B and Matthay KK. Advancing therapy for neuroblastoma. Nat Rev Clin Oncol 2022; 1-19.
2. Otte J, Dyberg C, Pepich A, and Johnsen JI, MYCN Function in Neuroblastoma Development. Front Oncol 2021; 10: 3210.
3. Foster JH, Voss SD, Hall DC, Minard CG, Balis FM, Wilner K, et al. Activity of Crizotinib in Patients with ALK-Aberrant Relapsed/Refractory Neuroblastoma: A Children's Oncology Group Study (ADVL0912). Clin Cancer Res 2021; 27(13): 3543-8.
4. Carter YM, Kunnimalaiyaan S, Chen H, Gamblin TC, Kunnimalaiyaan M. Specific glycogen synthase kinase-3 inhibition reduces neuroendocrine markers and suppresses neuroblastoma cell growth. Cancer Biol Ther 2014; 15(5): 510-5.
5. Dickey A, Schleicher S, Leahy K, Hu R, Hallahan D, Thotala DK. GSK-3β inhibition promotes cell death, apoptosis, and in vivo tumor growth delay in neuroblastoma Neuro-2A cell line. J Neurooncol 2011; 104(1): 145-53.
6. Augello G, Emma MR, Cusimano A, Azzolina A, Montalto G, McCubrey JA, Cervello M. The Role of GSK-3 in Cancer Immunotherapy: GSK-3 Inhibitors as a New Frontier in Cancer Treatment. Cells 2020; 9(6): 1427.
7. Arciniegas Ruiz SM, Eldar-Finkelman H. Glycogen Synthase Kinase-3 Inhibitors: Preclinical and Clinical Focus on CNS-A Decade Onward. Front Mol Neurosci 2022; 14: 792364.
8. Peres ALGL, Soares JS, Tavares RG, Righetto G, Zullo MAT, Mandava NB, Menossi M. Brassinosteroids, the Sixth Class of Phytohormones: A Molecular View from the Discovery to Hormonal Interactions in Plant Development and Stress Adaptation. Int J Mol Sci 2019; 20(2): 331.
9. Thummel CS, Chory J. Steroid signaling in plants and insects-common themes, different pathways. Genes Dev 2002; 16(24): 3113-29.
10. Manghwar H, Hussain A, Ali Q, Liu F. Brassinosteroids (BRs) Role in Plant Development and Coping with Different Stresses. Int J Mol Sci 2022; 23(3): 1012.
11. Kaur Kohli S, Bhardwaj A, Bhardwaj V, Sharma A, Kalia N, Landi M, Bhardwaj R. Therapeutic Potential of Brassinosteroids in Biomedical and Clinical Research. Biomolecules 2020; 10(4): 572.
12. Steigerova J, Rarova L, Oklestkova J, Krizova K, Levkova M, Svachova M, et al. Mechanisms of natural brassinosteroid-induced apoptosis of prostate cancer cells. Food Chem Toxicol 2012; 50(11): 4068-76.
13. Coskun D, Obakan P, Arisan ED, Çoker-Gürkan A, Palavan-Ünsal N. Epibrassinolide alters PI3K/MAPK signaling axis via activating Foxo3a-induced mitochondria-mediated apoptosis in colon cancer cells. Exp Cell Res 2015; 338(1): 10-21.
14. Obakan P, Arisan ED, Calcabrini A, Agostinelli E, Bolkent S, Palavan-Unsal N. Activation of polyamine catabolic enzymes involved in diverse responses against epibrassinolide-induced apoptosis in LNCaP and DU145 prostate cancer cell lines. Amino Acids 2014; 46(3): 553-64.
15. Johnsen JI, Dyberg C, Wickström M. Neuroblastoma-A Neural Crest Derived Embryonal Malignancy. Front Mol Neurosci 2019; 12: 9.
16. Gao Y, Tan L, Yu JT, Tan L. Tau in Alzheimer's Disease: Mechanisms and Therapeutic Strategies. Curr Alzheimer Res 2018; 15(3): 283-300.
17. Steigerova J, Oklestkova J, Levkova M, Rarova L, Kolar Z, Strnad M. Brassinosteroids cause cell cycle arrest and apoptosis of human breast cancer cells. Chem Biol Interact 2010; 188 (3): 487-96.
18. Obakan P, Barrero C, Coker-Gurkan A, Arisan ED, Merali S, Palavan-Unsal N. SILAC-Based Mass Spectrometry Analysis Reveals That Epibrassinolide Induces Apoptosis via Activating Endoplasmic Reticulum Stress in Prostate Cancer Cells. PLoS One 2015; 10(9): e0135788.

19. Bravo R, Parra V, Gatica D, Rodriguez AE, Torrealba N, Paredes F, et al. Endoplasmic reticulum and the unfolded protein response: dynamics and metabolic integration. Int Rev Cell Mol Biol 2013; 301: 215-90.
20. Adams CJ, Kopp MC, Larburu N, Nowak PR, Ali MMU. Structure and Molecular Mechanism of ER Stress Signaling by the Unfolded Protein Response Signal Activator IRE1. Front Mol Biosci 2019; 6: 11.
21. Nie T, Yang S, Ma H, Zhang L, Lu F, Tao K, et al. Regulation of ER stress-induced autophagy by GSK3β-TIP60-ULK1 pathway. Cell Death Dis 2016; 7(12): e2563.
22. Beurel E, Grieco SF, Jope RS. Glycogen synthase kinase-3 (GSK3): regulation, actions, and diseases. Pharmacol Ther 2015; 148: 114-31.
23. Wu D, Pan W. GSK3: a multifaceted kinase in Wnt signaling. Trends Biochem Sci 2010; 35(3): 161-8.
24. Zhang C, Su L, Huang L, Song ZY. GSK3β inhibits epithelial-mesenchymal transition via the Wnt/β-catenin and PI3K/Akt pathways. Int J Ophthalmol 2018; 11(7): 1120-8.
25. Kourtidis A, Lu R, Pence LJ, Anastasiadis PZ. A central role for cadherin signaling in cancer. Exp Cell Res 2017; 358(1): 78-85.
26. Donmez HG, Demirezen S, Beksac MS. The relationship between beta-catenin and apoptosis: A cytological and immunocytochemical examination. Tissue Cell 2016; 48(3): 160-7.
27. Martinez-Font E, Pérez-Capó M, Ramos R, Felipe I, Garcías C, Luna P, et al. Impact of Wnt/β-Catenin Inhibition on Cell Proliferation through CDC25A Downregulation in Soft Tissue Sarcomas. Cancers (Basel) 2020; 12(9): 2556.
28. Lee Y, Lee JK, Ahn SH, Lee J, Nam DH. WNT signaling in glioblastoma and therapeutic opportunities. Lab Invest 2016; 96(2): 137-50.
29. Meares GP, Mines MA, Beurel E, Eom TY, Song L, Zmijewska AA, Jope RS. Glycogen synthase kinase-3 regulates endoplasmic reticulum (ER) stress-induced CHOP expression in neuronal cells. Exp Cell Res 2011; 317(11): 1621-8.
30. Obakan Yerlikaya P, Arısan ED, Coker Gurkan A, Okumus OO, Yenigun T, Ozbey U, Kara M, Palavan Unsal N. Epibrassinolide prevents tau hyperphosphorylation via GSK3β inhibition in vitro and improves Caenorhabditis elegans lifespan and motor deficits in combination with roscovitine. Amino Acids 2021; 53(9): 1373-89.
31. Liao Y, Sassi S, Halvorsen S, Feng Y, Shen J, Gao Y, Cote G, et al. Androgen receptor is a potential novel prognostic marker and oncogenic target in osteosarcoma with dependence on CDK11. Sci Rep 2017; 7: 43941.
32. Wang Y, Mikhailova M, Bose S, Pan CX, deVere White RW, Ghosh PM. Regulation of androgen receptor transcriptional activity by rapamycin in prostate cancer cell proliferation and survival. Oncogene 2008; 27(56): 7106-17.
33. Bhutani KK, Paul AT, Fayad W, Linder S. Apoptosis inducing activity of steroidal constituents from Solanum xanthocarpum and Asparagus racemosus. Phytomedicine 2010; 17(10): 789-93.
34. Olivieri G, Baysang G, Meier F, Müller-Spahn F, Stähelin HB, Brockhaus M, Brack C. N-acetyl-L-cysteine protects SHSY5Y neuroblastoma cells from oxidative stress and cell cytotoxicity: effects on beta-amyloid secretion and tau phosphorylation. J Neurochem 2001; 76(1): 224-33.
35. Obakan P, Arisan ED, Coker-Gurkan A, Palavan-Unsal N. Epibrassinolide-induced apoptosis regardless of p53 expression via activating polyamine catabolic machinery, a common target for androgen sensitive and insensitive prostate cancer cells. Prostate 2014; 74(16): 1622-33.
36. Petit-Paitel A, Brau F, Cazareth J, Chabry J. Involvment of cytosolic and mitochondrial GSK-3beta in mitochondrial dysfunction and neuronal cell death of MPTP/MPP-treated neurons. PLoS One 2009; 4(5): e5491.
37. Kotliarova S, Pastorino S, Kovell LC, Kotliarov Y, Song H, Zhang W, et al. Glycogen synthase kinase-3 inhibition induces glioma cell death through c-MYC, nuclear factor-kappaB, and glucose regulation. Cancer Res 2008; 68(16): 6643-51.
38. Kuwahara A, Sakai H, Xu Y, Itoh Y, Hirabayashi Y, Gotoh Y. Tcf3 represses Wnt-β-catenin signaling and maintains neural stem cell population during neocortical development. PLoS One 2014; 9(5): e94408.
39. Sadot E, Geiger B, Oren M, Ben-Ze'ev A. Down-regulation of beta-catenin by activated p53. Mol Cell Biol 2001; 21(20): 6768-81.
40. Jang GB, Kim JY, Cho SD, Park KS, Jung JY, Lee HY, et al. Blockade of Wnt/β-catenin signaling suppresses breast cancer metastasis by inhibiting CSC-like phenotype. Sci Rep 2015; 5: 12465.
41. Zhang L, Cheng H, Yue Y, Li S, Zhang D, He R. H19 knockdown suppresses proliferation and induces apoptosis by regulating miR-148b/WNT/β-catenin in ox-LDL -stimulated vascular smooth muscle cells. J Biomed Sci 2018; 25(1): 11.